

FINAL REPORT:

**Investigation of Laser Generation and Detection of Ultrasound in
Ceramic Matrix Composites and Intermetallics**

NASA Grant No. NAG3-1964

APRIL 1998

**Michael J. Ehrlich
Johns Hopkins University
Department of Materials Science and Engineering
102 Maryland Hall
3400 North Charles Street
Baltimore, MD 21218
Telephone: 410-516-8660
E-mail: mehrlich@jhu.edu**

FINAL REPORT – NASA GRANT NAG3-1964

Investigation of Laser Generation and Detection of Ultrasound in Ceramic Matrix Composites and Intermetallics

Dr. Michael J. Ehrlich
Johns Hopkins University
Baltimore, MD 21218

21-April-1998

Objective

The goal of this program is to assess the feasibility of using laser based ultrasonic techniques for inspecting and characterizing materials of interest to NASA, specifically those used in propulsion and turbomachinery applications, such as ceramic composites, metal matrix composites, and intermetallics.

Relevancy

This work has direct benefit in both the civilian and government sectors. New propulsion and turbomachinery designs are utilizing advanced materials such as ceramic composites, metal matrix composites, and intermetallics to ever greater extents. Unlike more conventional materials, these new materials may be highly anisotropic and heterogeneous. The defect rate for many of these advanced material structures is significant because of the relative infancy of the required processing technology. For this reason, many of these structures are inspected immediately after manufacture. However, owing to material anisotropy and heterogeneity, and the fact that many new structures are manufactured with intricate contours, inspection is rarely straightforward and the results are often difficult to interpret. In-service inspection of these structures is also problematic, as often only single-sided access is permitted, and highly contoured parts may prove un-inspectable with current technology. The work performed under this program is aimed at assessing the feasibility of using a relatively new technique, laser based ultrasonics, for inspection and characterization of these types of materials and structures.

Background

Laser based systems for generation and detection of ultrasound have been investigated widely in academic and industrial laboratories around the world. These promising techniques offer noncontact and remote means for ultrasonic inspection of materials and structures. Since light beams from a laser are all that must come in “contact” with the surface of an object under inspection, prospects for high scan rates and inspection of surfaces with complex contours add to the attractiveness of this technology. In addition to the potential advantages for inspection of manufactured materials and structures in service, laser generation and detection of ultrasound is also being targeted at process control applications where measurements can be made on hot materials or those under high pressure or in otherwise hostile environments, so long as optical access to the material can be gained through an inspection port. Also, since ultrasonic transduction with laser beams can be done in the absence of couplants and without being subjected to the mechanical resonances associated with most contact ultrasonic transducers, laser

based methods are capable of sensing ultrasonic vibrations with extreme fidelity, opening possibilities for data interpretation beyond simple time-of-flight and attenuation measurements currently made with conventional piezoelectric ultrasonic transducers.

Unfortunately, laser based ultrasonic systems suffer from considerably poorer sensitivity than their conventional counterparts. The factors affecting performance of the receiver systems are well understood; however, less well understood are those parameters associated with the mechanism for laser generation of the ultrasound. Put simply, the signal-to-noise ratio for a laser ultrasonic system is directly proportional to the power of the receiving laser, the ultrasonic surface displacement, and inversely proportional to the total system bandwidth. The last two of these factors, surface displacement and system bandwidth, pertain almost exclusively to the laser generation side of the system. The ultrasonic signal generated by a laser source depends on the thermal, optical, and elastic properties of the specimen and on the characteristics of the laser source. For a given materials system, the laser source parameters, including temporal profile, spatial profile, energy, and wavelength, can be chosen such that the signal-to-noise ratio of the laser ultrasonic system is maximized.

A typical laser-based ultrasonic inspection system utilizes a nanosecond pulsed laser to locally heat the material of interest, causing a rapid thermal expansion which generates propagating ultrasonic waves within the material. The ultrasonic waves propagate into the material and interact with internal defects, structures, voids, layer interfaces, etc.. An optical interferometer is then used to sense the surface displacements caused by the ultrasonic waves after they have interrogated the material. The optical interferometers used are most often either Michelson or Fabry-Perot types, and characteristically have diffraction limited spatial resolution.

Unlike conventional ultrasonics, where a transducer is used to generate ultrasound which is subsequently coupled into the material of interest, laser ultrasonics uses no such transducer. Rather, it is the material itself which acts as a transducer and to a large extent governs the efficiency and characteristics of ultrasound generation. The ultrasound is generated when optical energy from the source laser is absorbed at or slightly below the material's surface. Absorption of the optical energy causes a rapid, local temperature rise, which, through thermal expansion, produces steep stress gradients within the material. These stress gradients propagate through the material as ultrasonic waves.

Since the material itself acts as the transducer, the efficiency and characteristics of the laser generation process are governed by material properties such as optical absorption coefficient, thermal conductivity, and coefficient of thermal expansion. As these properties vary considerably from one material to another, so too does the laser generation process. Owing to this, it is important to characterize each material of interest.

Results

Two material samples were received from NASA for characterization. The first was a metal matrix composite, consisting of a titanium alloy matrix (Ti-15-3) surrounding an array of unidirectional silicon carbide (SiC) fibers. The second sample was monolithic SiC. Results from the titanium metal matrix composite will be discussed first.

Titanium Metal Matrix Composite (MMC)

Laser based ultrasound studies were performed on the MMC supplied by NASA. Initially, two sides of the MMC were polished so that ultrasound detection could be accomplished using a high

fidelity, broad bandwidth Michelson interferometer. A schematic of the experimental setup is shown in Figure 1:

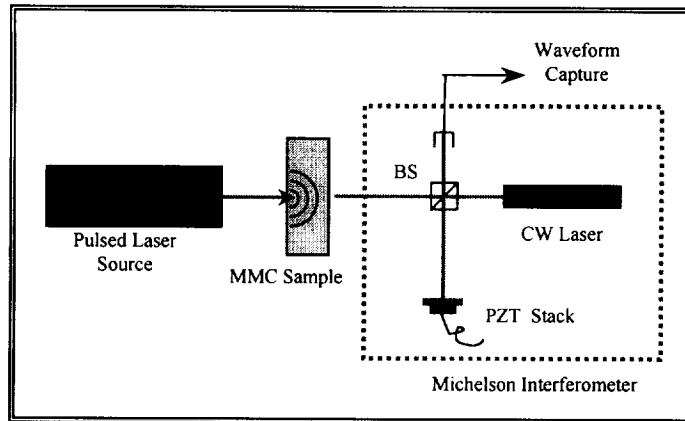


Figure 1. Schematic of experimental setup for laser generation and detection of ultrasound.

For all experiments, the direction of propagation of the ultrasound was perpendicular to the SiC fiber direction. A typical laser generated / laser detected signal for the MMC is shown in Figure 2. The large spike at $t=0 \mu\text{s}$ is the trigger pulse. The first arrival of the through-transmitted longitudinal wave arrives at approximately $3.28 \mu\text{s}$, and is followed by substantial scatter owing to the presence of the SiC fiber. In fact, the shear arrival and multiple longitudinal reflections are completely obscured by the scattered ultrasound. It is interesting to compare the MMC signal with that obtained from a solid piece of Ti-1-7 alloy with no SiC fibers. These results are shown in Figure 3. For the solid Ti-1-7, the first longitudinal arrival is evident at approximately $4 \mu\text{s}$, with four additional multiple reflections clearly visible.

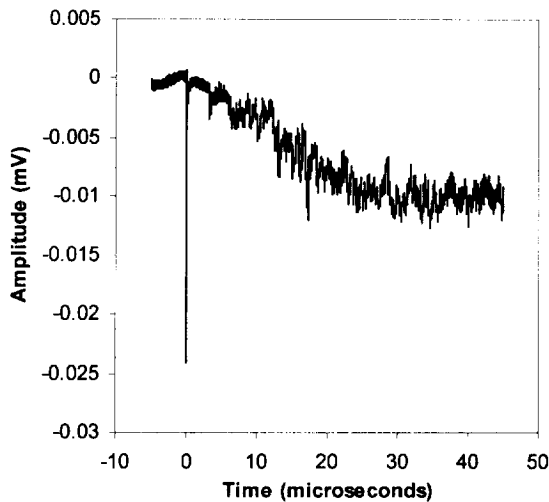


Figure 2. Typical laser ultrasonic signal obtained from the Ti-MMC

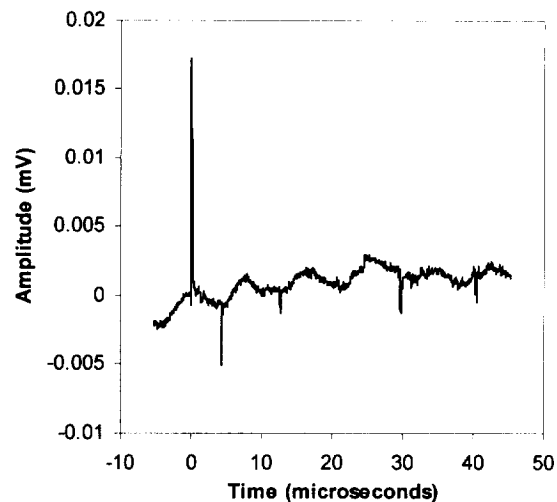


Figure 3. Laser ultrasonic signal obtained from solid Ti-1-7 with no SiC fibers.

It should be pointed out here that the tremendous scatter arising from the presence of the SiC fibers does not bode well for laser based ultrasonic inspection of such materials. For single sided inspections, the scattered field would likely completely mask any defect arrivals, and would certainly make defect classification based on frequency analysis extremely difficult. Shown in Figures 4 and 5 below are the associated frequency spectra of the Ti-MMC and Ti-1-7 laser ultrasonic signals.

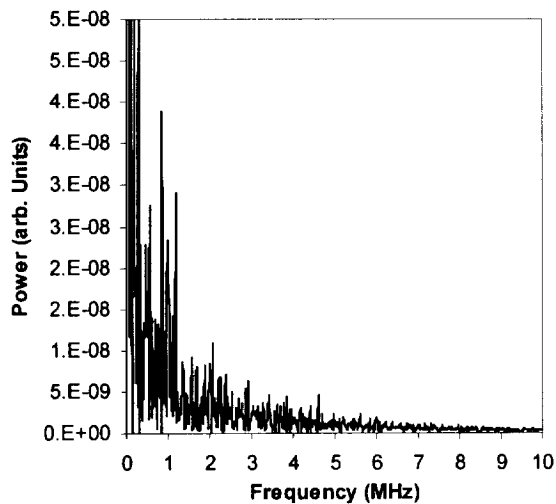


Figure 4. Frequency spectrum of the Ti-MMC laser ultrasonic signal.

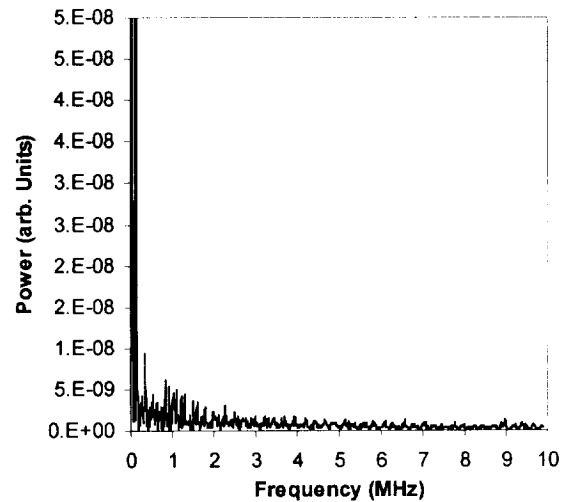


Figure 5. Frequency spectrum of the solid Ti-1-7 laser ultrasonic signal.

It is clear from these figures that the frequency spectrum of the transmitted laser ultrasonic signal has substantially more noise energy content out to approximately 3 MHz than that of the solid sample. Again, this scattered field manifests itself as noise over the 0-3 MHz range. Since the laser ultrasonic receiver is a point receiver and is not focused in any manner, it would be extremely difficult to perform defect detection in a single sided inspection scenario. Even amplitude based through-transmission inspection may be difficult to perform, because of the non-uniformity of fiber placement in these materials. Regions with more fiber may tend to scatter more than other regions, etc.

In an effort to determine if the non-uniformity of fiber placement in these MMC's was observable using the laser based technique, a 1 cm square section was scanned in a through transmission mode with a point spacing of 500 μm using a laser-based ultrasonic C-scan system. Again, the direction of sound propagation was perpendicular to the fiber direction. A cross section of the fiber placement in this geometry reveals that the fibers are more densely packed near the center of the sample than toward the edges. The geometry of the scan is shown in Figure 6.

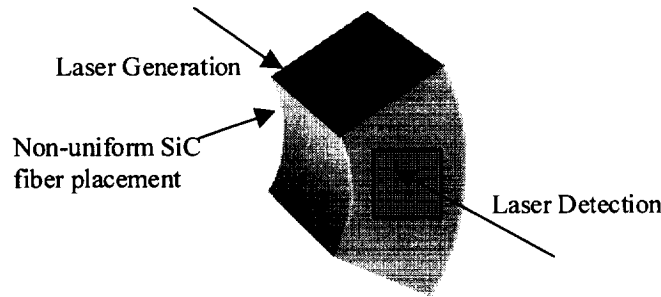


Figure 6. Geometry for through transmission C-scan of Ti-MMC. SiC fibers run along the curve of the part, and are packed considerably more dense in the center.

Typical data from 20 locations in a single row across the sample are shown in a waterfall plot in Figure 7. This same data is represented as a greyscale image in Figure 8, since it is often easier to pick out waveform features in this type of representation. The dark vertical line at $2.5 \mu\text{s}$ is the through-transmitted longitudinal wave arrival. Progressing farther in time, two white lines are seen which arc away from the first longitudinal arrival and cross at the center point of the sample. It is believed that these lines represent longitudinal arrivals for waves which have reflected off the sides of the specimen. The last clear features in the waveforms are the dark lines which also arc toward later times near the center of the sample. It is believed that these are mode-converted shear waves which have reflected off the sides of the sample. Again, these are data from one of twenty rows across the sample.

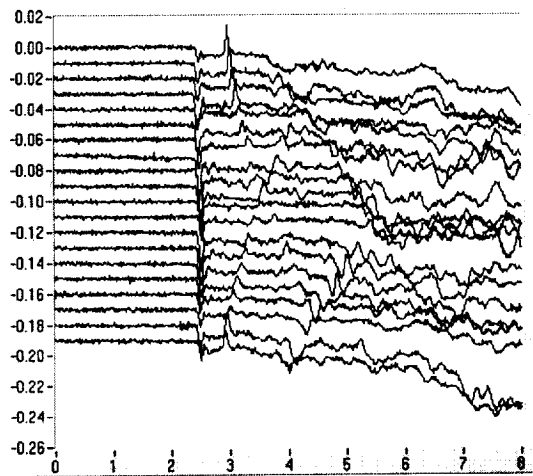


Figure 7. Waterfall plot of laser ultrasonic waveforms from one row of the C-scan. Each of twenty separate signals are stacked upon each other.

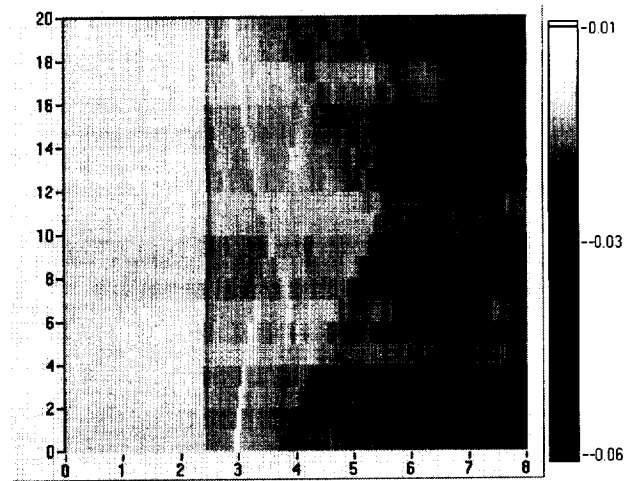


Figure 8. Greyscale representation of the data displayed in Figure 7.

These figures also give an excellent example of multi-path problems when inspecting with laser ultrasound. Unlike a conventional transducer, which generates a relatively narrow and minimally diverging beam of ultrasound, the sound front generated by a laser source diverges to a much greater extent, and therefore may be problematic near the edges of parts.

The change in time-of-flight of the through-transmitted longitudinal wave as a function of position on the sample for the C-scan described above is shown in Figure 9. Bright regions indicate slower overall velocities, while dark regions indicate faster velocities. As seen in Figure 9, there is a bright vertical region in the center of this area where the overall longitudinal velocity was somewhat less than in the surrounding area. In this region of the sample, the SiC fibers are more densely packed than in the surrounding region. Because of this, there is considerably more SiC-free titanium alloy near the front and back surfaces. Based on these results, it would appear that the velocity measurement is sensitive to fiber uniformity in the part. Again, however, it is unlikely that a single sided inspection would provide useful defect location owing to the strong scattering by the SiC fibers.

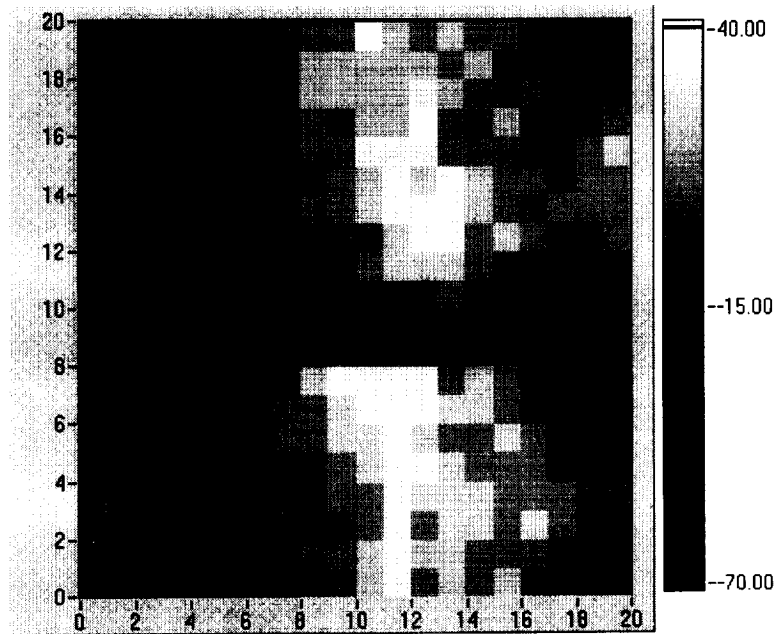


Figure 9. Change in time-of-flight data for the Ti-MMC based on a laser ultrasonic C-scan of the part.

Also, because of the multipath problem described above given the sample of relatively small size, directivity measurements were difficult to accomplish. Included here for reference are measurements made of directivity and ultrasonic amplitude, under a separate program, for an ablative laser source taken in the solid Ti-1-7 alloy which was 25 mm thick. It is expected that results for the Ti-15-3 MMC would be similar. Figure 10 plots the longitudinal wave amplitude as a function of distance off epicenter for the 25 mm thick Ti-1-7 alloy. As seen, the ultrasonic wave amplitude has dropped to just less than one-third of its epicentral value at 45° (25 mm off epicenter). This broadly divergent source characteristic is problematic in small samples and leads to the multipath noise described earlier. Figure 11 shows the dependence of the ultrasonic wave amplitude on incident power density for 500 μm and 785 μm source spot sizes. As expected, the longitudinal amplitude increases with increasing power density.

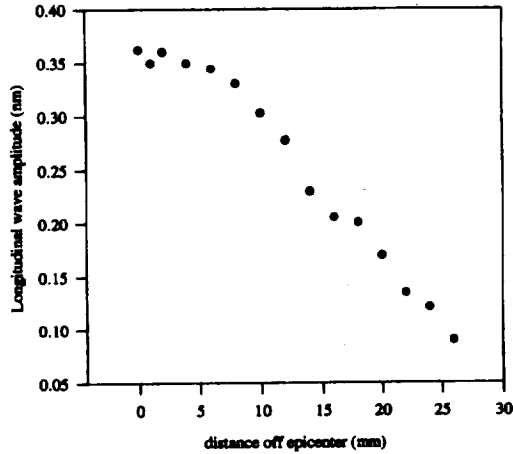


Figure 10. Longitudinal wave directivity for laser generated ultrasound in Ti-1-7 for a 25mm thick sample.

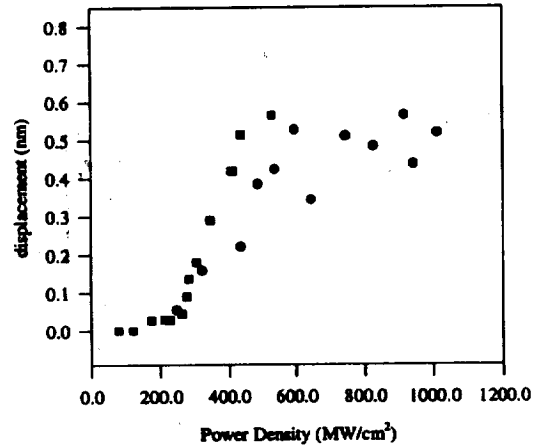


Figure 11. Surface displacement as a Function of power density for laser generated ultrasound through 25mm of solid Ti-1-7. Circles are for 500 µm and squares for 785 µm spot size.

Monolithic Silicon Carbide

The monolithic SiC sample received from NASA for laser ultrasonic testing was approximately 25 mm long by 5 mm wide by 2 mm thick. As described earlier, small samples inspected with laser based ultrasonics can lead to significant multi-path problems. Nonetheless, the SiC sample was subjected to both thermoelastic and ablative laser sources, and a Michelson interferometer was used to detect the ultrasonic arrivals. Typical ultrasonic signals from the SiC are shown in Figures 12 and 13, for a thermoelastic and ablative source, respectively.

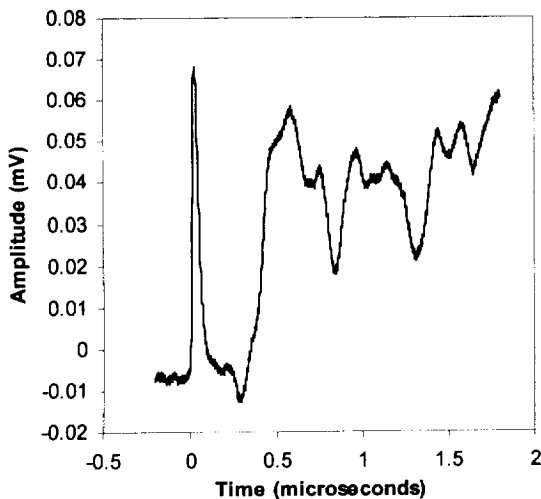


Figure 12. Thermoelastic waveform for SiC sample.

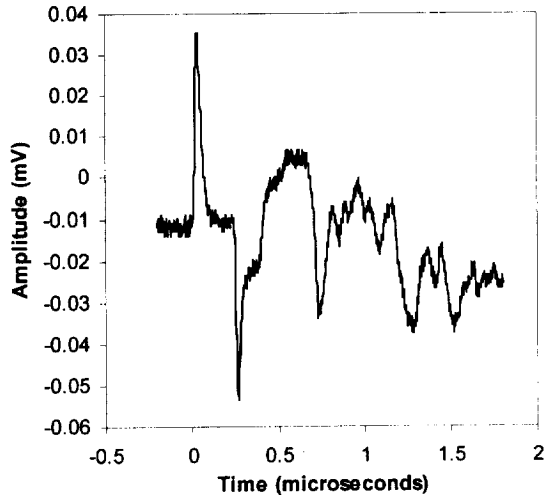


Figure 13. Ablative waveform for SiC sample.

Both the thermoelastic and ablative waveforms show the trigger pulse at $t=0 \mu\text{s}$ and the first longitudinal arrival at approximately 300 ns. This arrival is considerably stronger for the ablative case. Also, multiple reflections of the longitudinal wave are evident for both cases. One point to note here is that for the ablative case, it appears that the multiple reflections become increasingly broad (loss of high frequency content). It is believed at this time that this effect is not material dependent, but rather geometry dependent and a function of multi-path in the small sample sizes. Also shown for completeness are the frequency spectra for each signal in Figures 14 and 15. As evident, there appears to be little difference in the frequency content between the thermoelastic and ablative signals, however there is a slight increase in higher frequency content in the ablative signal.

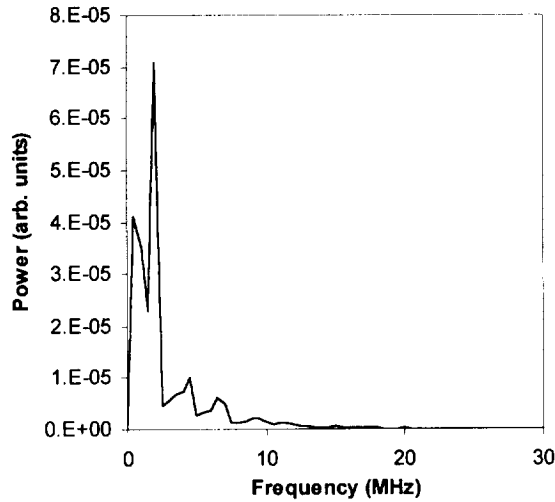


Figure 14. Frequency spectrum for a laser generated thermoelastic signal in SiC.

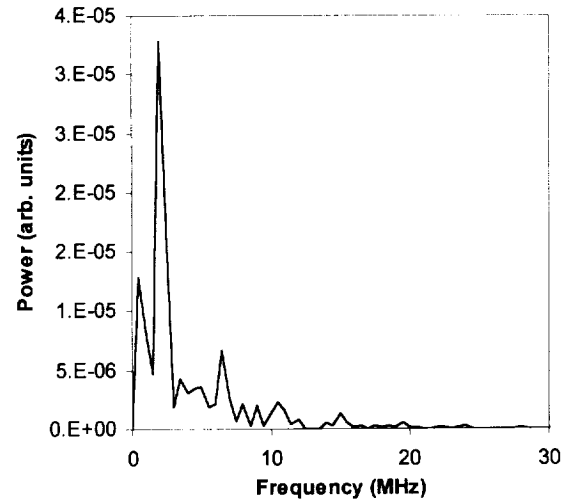


Figure 15. Frequency spectrum for a laser generated ablative signal in SiC.